Catalysis Today 164 (2011) 325–331

Contents lists available at ScienceDirect

Catalysis Today

journal homepage: www.elsevier.com/locate/cattod

Specific role of polymorphs of supporting titania in catalytic CO oxidation on gold

A. Beck[a], G. Magesh[b], B. Kuppan[b], Z. Schay[a], O. Geszti[c], T. Benkó[a], R.P. Viswanath[b], P. Selvam[b], B. Viswanathan[b], L. Guczi[a,d,*]

[a] Department of Surface Chemistry and Catalysis, Institute of Isotopes, HAS, P.O. Box 77, H-1525 Budapest, Hungary
[b] National Centre for Catalysis Research, Department of Chemistry, Indian Institute of Technology Madras, Chennai 600 036, India
[c] Research Institute for Technical Physics and Materials Science, HAS, Konkoly Thege Miklós út 29/33, H-1525 Budapest, Hungary
[d] Chemical Research Center, Institute of Nanochemistry and Catalysis, P.O. Box 17, H-1525 Budapest, Hungary

ARTICLE INFO

Article history:
Received 1 July 2010
Received in revised form
26 November 2010
Accepted 1 December 2010
Available online 14 January 2011

Keywords:
Gold catalysis
Brookite
Perimeter
CO oxidation

ABSTRACT

Dependence of catalytic activity in CO oxidation on the structure of gold nanoparticles supported on various TiO_2 polymorphs has been investigated. Pure brookite, brookite–anatase (45:55) and anatase–rutile (85:15) mixtures were compared as supports of Au/TiO_2. Au nanoparticles were deposited on different TiO_2 supports by adsorption of Au colloids of about 6 and 15 nm mean diameter and by deposition precipitation (DP) with urea providing Au particles smaller than 5 nm in size. Sol derived gold particles were more stable against sintering on brookite than on anatase containing supports. Taking into account the particle sizes of gold and titania for all types of gold deposition methods, the Au–anatase perimeter seems to be significantly more active in CO oxidation than the Au–brookite perimeter. The difference in activity should be originated from the different electronic, physical and surface properties of anatase and brookite.

1. Introduction

It has been a wide scale of research for TiO_2 as support for Au nanoparticles catalysing CO oxidation. The different polymorphs of a compound have a large variation in their properties. TiO_2 has three different crystal structures, namely anatase, rutile (both tetragonal) and brookite (orthorhombic), which have different photocatalytic properties because of the variation in the energy of band gaps [1–3]. The band gaps of anatase, brookite and rutile are 3.05, 3.26 and 2.98 eV respectively. In addition, the potential of the bottom of the conduction band of anatase, rutile and brookite are at −0.45, −0.46 and −0.37 vs NHE, respectively. Variation in the photocatalytic properties of these allotropic forms of TiO_2 were explained successfully based on the above points. It is also known that brookite and anatase transform to the rutile phase at 800 °C and 915 °C respectively. The surface enthalpy follows the order rutile ($2.2 \pm 0.2\ J\ m^{-2}$) > brookite ($1.0 \pm 0.2\ J\ m^{-2}$) > anatase ($0.4 \pm 0.2\ J\ m^{-2}$) [4]. These variations in the properties of the allotropic forms are expected to influence the catalytic activity, when they are used as supporting material for gold.

Meanwhile, gold, that was considered earlier as a highly inactive metal as a catalyst was found to be active when present in nanometer sized particles [5,6]. Various supports have been used for gold nanoparticles of the same size and used for promoting the catalytic CO oxidation. Among TiO_2, Al_2O_3, CeO_2, ZnO, SiO_2, ZrO_2, and Co_3O_4 as supports TiO_2, Co_3O_4 and Al_2O_3 were found to be the most active [7–9]. Comotti et al. [8] reported the CO oxidation activity of samples prepared by colloidal deposition method, where pre-synthesized gold nanoparticles of uniform size were deposited on different supports, the activity followed the sequence of $TiO_2 > Al_2O_3 > ZnO > ZrO_2$. These results show that the support plays a significant role in deciding the CO oxidation activity of the catalyst. The different morphology of given oxide may also affect the activity as was reported for TiO_2 promoted Au/SiO_2 catalysts. The highly dispersed, mainly amorphous TiO_2 formed a perimeter with gold which was more active than the perimeter of Au with crystalline anatase [10–12].

There are other factors which have been reported to influence the catalytic activity. They are size of the gold particles, oxidation state (cationic sites) of gold species [13,14], and the preparation method [15–19]. In addition, low-coordinated step and corner atoms [20–23], metal–support interface area [6,24–26], and the charge transfer from the support to the metal [27,28] are also reported to influence the activity.

Most of the CO oxidation studies were carried out using anatase and rutile phases of TiO_2 as support for Au. Systematic compar-

* Corresponding author at: Department of Surface Chemistry and Catalysis, Institute of Isotopes, HAS, P. O. Box 77, H-1525 Budapest, Hungary.
E-mail address: guczi@mail.kfki.hu (L. Guczi).

0920-5861/$ – see front matter © 2010 Elsevier B.V. All rights reserved.
doi:10.1016/j.cattod.2010.12.006

ison on the effect of different titania polymorphs was reported only in several papers [29–32]. The results indicated that anatase is a better support than rutile and the thermal stability of rutile supported catalysts is less compared to that of anatase. Studies using brookite as support for gold were not carried out extensively so far. Yan et al. [31,32] recently reported the brookite phase to be more active towards CO oxidation than anatase and rutile forms of TiO_2. The brookite as support was described to prevent more efficiently the sintering of the gold nanoparticles than the anatase and rutile forms of TiO_2. However, the report by Yan et al. is based on the results from the deposition–precipitation method, where the support considerably influences the particle size and shape of the particles of Au. Among the various methods of preparation of supported gold nanoparticles described, deposition precipitation methods are reported to yield the most active catalysts [33–35]. However, for comparing the effect of the various supports on the metal and subsequently the catalytic activity, deposition–precipitation method may not be reliable. With the different sizes and shapes of gold on different supports, the variation in the activity of the different catalysts cannot be attributed specifically to the interaction between the support and gold. This led us to prepare catalysts by sol deposition method where same size and shaped gold particles were prepared separately and then deposited on the different support. Furthermore, this method leads to uniform weight loading of gold on the various supports.

The issue on which the literature is silent is: how does the brookite–metal interaction differ from that of anatase or rutile–metal interaction concerning the CO oxidation activity? In order to obtain appropriate answer to this question, brookite has been prepared by two different methods and compared with anatase and rutile containing Degussa P25 type TiO_2 as supports of gold in catalytic CO oxidation. Gold was deposited with similar loadings by sol adsorption method and deposition–precipitation by urea (DPU).

2. Experimental

2.1. Preparation of TiO_2 from $TiCl_3$

TiO_2 was prepared using $TiCl_3$ (Loba Chemie) according to the procedure adopted by Lee et al. [36] as follows. Urea (0.5 M) was dissolved in 1000 ml of an aqueous solution containing titanium trichloride ($TiCl_3$, 0.015 M). The resulting solution was refluxed at 100 °C for 7 h while stirring leading to the formation of cream coloured precipitate. The precipitate was separated by centrifuging and washing repeatedly (four times with de-ionized water and once with anhydrous ethanol). The precipitated powders were then dried at 100 °C for 2 h in an oven. TiO_2 prepared by this method is being denoted as BA.

2.2. Preparation of TiO_2 from $TiCl_4$

Additionally, TiO_2 was also prepared by following the previously reported method [37]. 0.15 M $TiCl_4$ (99% purity, Merck) was added to 250 ml of 3 M HCl in a 500 ml sealed bottle and heated to 100 °C for 48 h. The obtained precipitate contained brookite and rutile TiO_2. The brookite phase was separated by peptization. The precipitate was dispersed in 3 M nitric acid and the resulting suspension was centrifuged. The solid phase obtained was dispersed in water and then centrifuged. The centrifugate was freeze dried to obtain pure brookite which was dried at 100 °C for 4 h. The TiO_2 prepared this way was denoted as B.

2.3. Preparation of Au/TiO_2 by sol method

40 ml of 5 mM aqueous $HAuCl_4$ solution (Sigma–Aldrich) was made up to 600 ml using bidistilled water. Another solution was made by mixing 32 ml 1% sodium citrate, 8 ml of 1% tannic acid and 120 ml of water. pH of the solution was adjusted to 8 using 4% sodium carbonate solution. The two solutions were heated separately to 60 °C under stirring, then mixed and maintained at 60 °C for 30 min under stirring. The solution turned deep red due to the formation of gold sol. Three sols were prepared denoted as SAu_{15}, SAu_6 and SAu_5.

Gold sols were adsorbed on the two types brookite containing TiO_2 prepared (BA, B) and on the commercial Degussa P25 TiO_2 composed of anatase and in smaller amount rutile (denoted as AR) by addition of poly (diallyldimethylammonium chloride) (PDDA). This polycation adsorbing on the support surface increased the attraction between the support and the colloid Au particles stabilised by negatively charged citrate-tannic acid shell [11]. The amount of PDDA solution (0.08 wt%) required for complete adsorption was different, 23, 35 and 20 ml/g support for AR, BA and B type TiO_2, respectively. The dispersion obtained was stirred magnetically for 90 min. The solution became colourless and the TiO_2 attained a purple colour due to the adsorption of gold nanoparticles. The resulting precipitate was washed with water and dried at 60 °C for 24 h. Using this method gold sols were loaded on to the three different types of TiO_2, BA, B and AR providing samples SAu_{15}/AR, SAu_{15}/BA, SAu_{15}/B and SAu_6/AR, SAu_6/BA and SAu_5/B. Based on calculations, the gold loading on these catalysts was 2 wt%.

2.4. Preparation of Au/TiO_2 by DPU method

Gold was deposited onto all three types of TiO_2 supports also by deposition precipitation with urea [38]. In a typical preparation 1 g of TiO_2 was suspended in 96 ml bidistilled water and 4 ml of 25 mM $HAuCl_4$ solution and 2.5 mg urea was added. The suspension was heated up to 80 °C during about 3 h and kept at this temperature for 2–4 h under stirring, while the pH raised up to 7.0–7.5. The sample was filtered, washed and dried at 60 °C overnight. The pH raise was significantly slower in case of B titania, than in case of AR and BA. That is why the preparation with B type titania was repeated. Similarly slow increase of pH was observed as in the first preparation. The samples produced are denoted as DPUAu/AR, DPUAu/BA, DPUAu/B_1 and DPUAu/B_2.

2.5. Sample characterisation

Crystalline phase composition of the prepared TiO_2 was analyzed by X-ray diffraction (XRD) (Rigaku D/max 2400 instrument, Ni-filtered Cu Kα radiation, λ = 1.5418 Å). The crystallite sizes of the different phases were calculated from the line broadening of the most intense reflections using the Scherrer equation. The surface of the supports was measured by BET technique. Gold loading on TiO_2 was confirmed partly by X-ray fluorescence spectroscopy and ICP-OES analysis (Model: Perkin Elmer Optima 5300 DV).

The size of gold and TiO_2 particles was studied by a Philips CM20 transmission electron microscope (TEM) operating at 200 kV equipped with energy dispersive spectrometer (EDS) for electron probe microanalysis. The aqueous suspensions of the samples were dropped on carbon-coated grid and after evaporating water the electron micrographs of the particles were taken. The gold particle size distribution was obtained by measuring the diameter of about 200–300 metal particles.

Oxidation states and relative surface concentrations of Au were determined by X-ray photoelectron spectroscopy (XPS) performed by a KRATOS XSAM 800 XPS machine equipped with an atmospheric reaction chamber. Spectra were taken on the “as prepared”

Table 1
Specific surface area, crystalline phases and sizes in the different TiO_2 samples.

TiO_2 supports	Specific surface area (m^2/g)	Phase composition	Crystallite size (nm)	Preparation
AR	55	Anatase, 85%	34 (A)	Degussa P25
		Rutile, 15%	52 (R)	
BA	197	Brookite, 45%	13 (B)	$TiCl_3$ + urea/100 °C
		Anatase, 55%	9 (A)	
B	114	Brookite, 100%	23 (B)	$TiCl_4$ + HCl/100 °C

samples and after catalytic tests. MgKα excitation was used. The binding energies were determined relative to Ti 2p at 458.8 eV. For the surface composition, signals of Au 4f, O 1s, Ti 2p, and C 1s were considered using the sensitivity factors given by the manufacturer.

The CO oxidation activity was measured in a plug flow reactor at atmospheric pressure connected to a quadrupole mass spectrometer (QMS). Temperature programmed reaction was performed at a ramp rate of 5 °C/min with a reaction mixture composed of 0.5 vol.% carbon monoxide, 9.5% oxygen, 52% helium and 38% argon. Typically 30 mg of sieved fraction of the catalyst was tested and 27.5 ml/min of reaction mixture flow rate was applied. Only the pure titania (AR and B) samples and the three SAu_{15}/TiO_2 catalysts were tested differently, 50 mg catalyst with 27.5 ml/min flow rate and 60 mg catalyst with 35 ml/min flow rate were applied, respectively. Heating and cooling cycles were repeated until the concordance in ion current vs temperature plot was achieved. Concordance was normally achieved in 3–4 cycles. The conversion was calculated on the basis of the CO_2 ion current ($m/e = 44$) from the mass spectrometer after making the appropriate corrections. The sol prepared samples were tested after an in situ calcination treatment in a mixture of 20% O_2 in Ar (12.5 ml/min) at 400 °C for 60 min (heating rate was 10 °C/min) to remove the organic residues from the catalysts. The DPU samples were tested in CO oxidation up to 150 °C without any treatment then kept at this temperature for 1 h and after cooling down two additional heating up-cooling down cycles were repeated. Subsequently, the DPU samples were calcined in situ the same way as the sol derived ones and tested again in the temperature programmed CO oxidation.

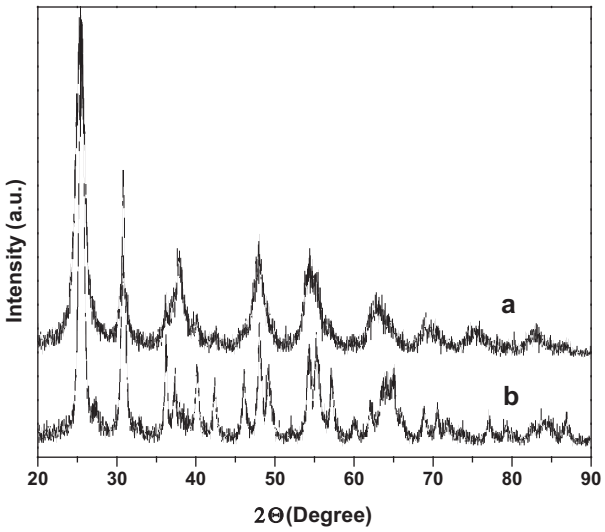

Fig. 1. XRD of BA (a) and B (b) type of TiO_2.

3. Results and discussion

3.1. BET, XRD and gold loading measurements

The surface area and the crystalline properties of the two types of TiO_2 prepared with those of the commercial titania were determined by the BET method and XRD measurements, respectively, and summarized in Table 1. The XRD of the TiO_2 prepared are shown on Fig. 1. The X-ray diffraction peaks of anatase and brookite appear very closely and were difficult to identify if both phases were present. Anatase phase of TiO_2 (JCPDS file no. 894921) has its diffraction peaks at 2θ values of 25.36, 37.85, 38.64, 48.15, 53.97, 55.19, 62.81, 70.46, and 75.20. Brookite phase of TiO_2 (JCPDS file no. 761936) gives diffraction peaks at 2θ values of 25.31, 30.75, 36.15, 37.22, 40.07, 42.26, 45.97, 49.06, 54.31, 55.14 and 61.95. X-ray diffraction analysis showed the presence of 100% brookite TiO_2 phase prepared from $TiCl_4$ that is why it is denoted by B. 55% anatase TiO_2 and 45% brookite TiO_2 were observed in the case of the sample prepared from $TiCl_3$ designated by BA. AR (Degussa P25 TiO_2) was composed of 85% anatase and 15% rutile according to our measurement. The crystalline phases did not change during the pretreatments and CO oxidation test according to the measurement of the used catalysts. The crystallite sizes in AR (34 nm for anatase and 53 nm for rutile) were much larger than those in the brookite containing BA and B. BA was composed of the smallest crystallites (9 nm anatase and 13 nm brookite), in TiO_2 type B 23 nm was the crystallite size. In agreement with the XRD size data, BET surface area analysis of B and BA showed surface area to be about 2 and 4 times higher than that of AR, 114 m^2/g and 197 m^2/g, respectively.

The gold loading of the samples are presented in Table 2. The real values agreed quite well with the intended 2 wt%. Sol deposition method provided samples of the same 2.2 wt% Au concentration, however the DPU preparations resulted also similar Au loading varying between 1.8 and 2.3 wt%.

3.2. TEM measurements

Fig. 2 shows representative images of the sol and DPU derived Au/TiO_2 samples after calcination treatment (400 °C/air/1 h). The size difference in the three TiO_2 supports can be seen very well in the micrographs. The mean particle sizes of gold and the standard deviations in the as prepared and the calcined catalysts are presented in Table 2. Surprisingly the sizes of the 3 Au sols prepared were different. Only one of them (SAu_6) contained particles of 6 nm average diameter as expected based on our earlier experiences [10]. Au particles in SAu_{15} were much larger (about 15 nm), in SAu_5 somewhat smaller (around 5 nm), than the 6 nm expected value. The reason of the differences should be the application of different quality water for the colloid formation. In the case of SAu_6 and SAu_{15} samples bidistilled water was applied, whose quality was accidentally not good in case of preparation of SAu_{15}. Therefore, for preparation of SAu_5 MilliQ water was used. The size distribution of SAu_{15} was wide, whereas the SAu_6 and SAu_5 were mostly monodisperse. The originally large Au particles in SAu_{15} were stable against sintering during calcination, while the smaller particles originated from SAu_6 and SAu_5 sintered to different extent on the 3 types of support. Au on pure brookite (B) was more stable than on the anatase containing supports (AR, BA). In the calcined DPU samples Au was highly dispersed and evenly distributed on the support. In DPUAu/AR and DPUAu/B Au was easily distinguishable from the larger TiO_2 particles, while for DPUAu/BA this was not the case. In the network of the small TiO_2 particles the small Au particles were

Table 2
Au loading and Au mean diameter determined by TEM in as prepared form and after calcination at 400 °C in air for 1 h in the different Au/TiO_2 samples.

Sample	Au loading (wt%)[a]	Au size in as prep. form (nm)	Au size after calcinations (nm)
SAu_{15}/AR	2.2	15.1 ± 5.5	15.0 ± 5.8
SAu_{15}/BA	2.2	n.m.	n.m.
SAu_{15}/B	2.2	15.2 ± 5.5	17.0 ± 6.4
SAu_6/AR	2.2	6.4 ± 1.4[b]	9.5 ± 6.3
SAu_6/BA	2.3	6.4 ± 1.4[b]	10.2 ± 9.4
SAu_5/B	2.1	4.7 ± 0.7[b]	5.9 ± 2.0
DPUAu/AR	1.8	n.m.	3.1 ± 0.8
DPUAu/BA	2.1	n.m.	5.0 ± 1.5
DPUAu/B_1	1.9	n.m.	2.9 ± 0.9
DPUAu/B_2	2.3	n.m.	n.m.

n.m. – not measured.
[a] Au loading of SAu_{15}/TiO_2 samples was determined by ICP-AES, all the other samples were measured by XRF.
[b] The size of gold particles was measured in the sol.

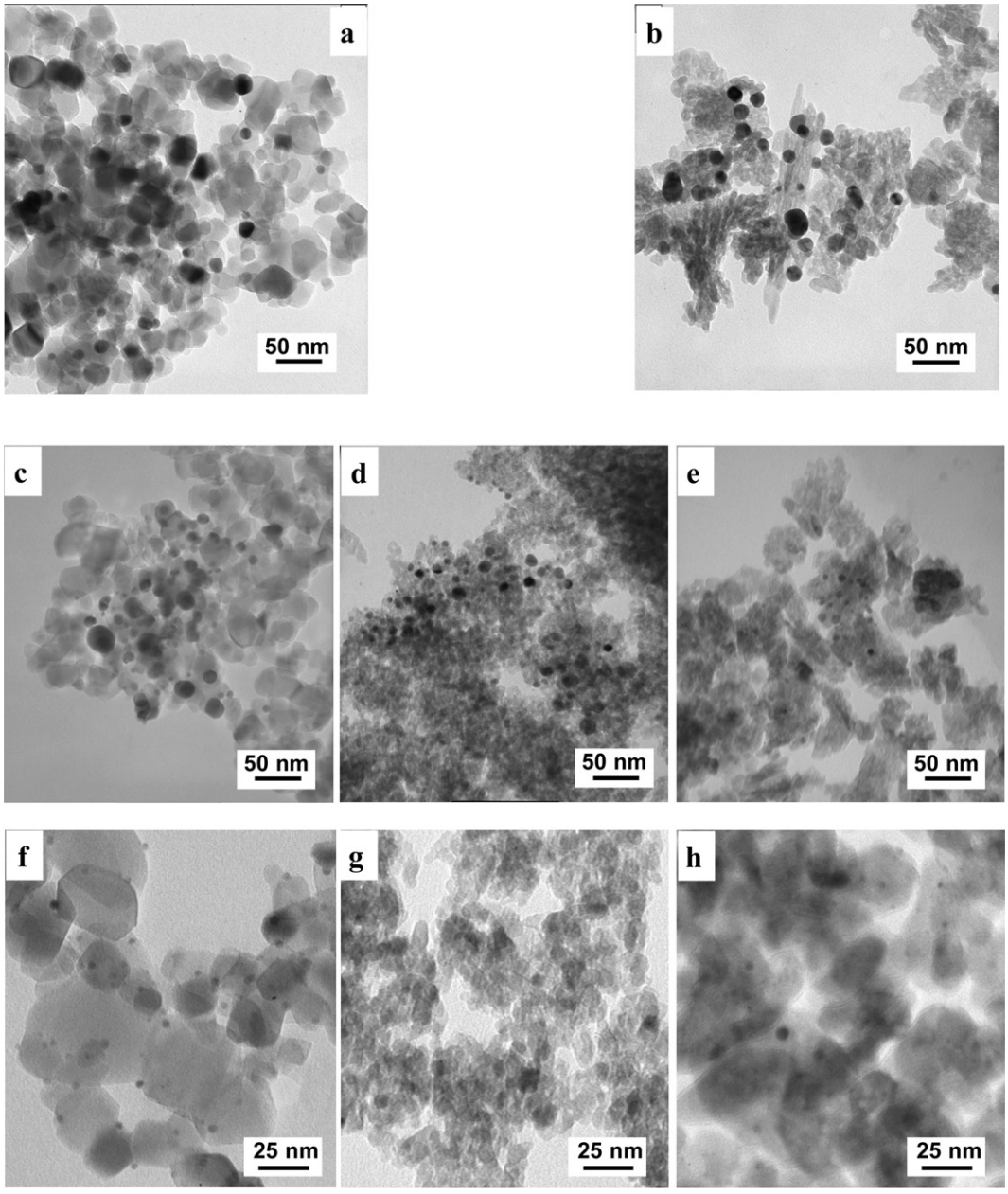

Fig. 2. TEM images of the different Au/TiO_2 samples after calcination at 400 °C in air for 1 h. (a) SAu_{15}/AR, (b) SAu_{15}/B, (c) SAu_6/AR, (d) SAu_6/BA, (e) SAu_5/B, (f) DPUAu/AR, (g) DPUAu/BA and (h) DPUAu/B.

Table 3
Relative surface concentrations and Au 4f binding energies in the different DPUAu/TiO_2 samples determined by XPS.

Samples	Au/Ti		C/Ti		O/Ti		Au 4f BE(eV)	
	As prep.	Used	As prep.	Used	As prep.	Used	As prep.	Used
DPUAu/AR	3.8%	0.7%	1.0	1.7	2.4	2.4	84.7	83.5
DPUAu/BA	1.3%	0.7%	0.4	1.5	2.5	2.8	85.0	83.9
DPUAu/BA 400 °C/air/1 h (in situ)	0.4%	–	0.4	–	2.4	–	83.8	–
DPUAu/BA 400 °C/H_2/1 h (in situ)	0.5%	–	0.1	–	2.4	–	84.0	–
DPUAu/B_1	1.6%	0.6%	1.6	2.0	2.6	2.9	84.7	83.6
DPUAu/B_2	1.6%	0.5%	1.0	1.3	2.5	2.5	84.6	83.7

hardly detectable and hence the mean diameter (5.0 ± 1.5 nm) may have been overestimated to some extent.

3.3. XPS studies

DPU prepared samples were characterised by XPS in as prepared state and after CO oxidation catalytic tests to study the surface concentrations and the Au $4f_{7/2}$ binding energy. The results are presented in Table 3. The Au/Ti atomic ratio at the surface in the as prepared samples were similar (1.3–1.6) except for DPUAu/AR which had 2–3 times higher Au/Ti ratio. During the pretreatments and catalytic tests the Au/Ti ratio significantly reduced on all DPU samples reaching Au/Ti ratio of 0.5–0.7. On the other hand, the C/Ti ratio increased and the O/Ti ratio did not show any change or increased slightly. Accordingly, sintering of gold and formation of some carbonaceous deposits on gold surface might have been taking place during catalytic tests. Effect of treatments on DPUAu/BA was also studied in situ in the atmospheric chamber attached to the XPS equipment. Au/Ti ratio decreased during the in situ calcination and reduction treatment, whereas the C/Ti ratio remained the same during air treatment and decreased during reduction. Thus, the increased surface concentration of carbon observed on the spent catalysts should be attributed to the effect of catalytic reaction.

In the as prepared DPU samples the binding energy of Au $4f_{7/2}$ (84.6–85.0 eV) was shifted to positive direction compared to the metallic Au by about 1 eV. The measured binding energy is typical for Au(I) compounds or this B.E. shift can be attributed to the presence of very small, d < 1–2 nm gold particles. In the as prepared state the DPU derived samples may have contained Au still in oxidised form. Tannic acid and citrate stabilised Au sol derived TiO_2 supported catalysts were studied earlier by XPS [39] and B.E. of gold showed typical metallic character, which is not surprising taking into account that the particles in sol were formed with liquid phase reduction. In the case of sol derived Au/TiO_2, the metallic state of gold changed neither in calcination nor in reductive treatment. In DPU prepared samples after catalytic measurements, in situ calcination and reduction treatment, Au was also in metallic state characterised by 83.5–84.0 eV B.E.

3.4. Catalytic CO oxidation

Catalytic CO oxidation were performed over the Au/TiO_2 catalysts prepared on 3 different phase compositions titania. There were 3 different particle size ranges (15–17, 6–10 and 3–5 nm) and two basically different Au deposition methods applied. The effect of the TiO_2 polymorphs on the CO oxidation activity of Au/TiO_2 could be studied depending on the Au size and preparation method. Temperature programmed CO oxidation conversion curves of the three types of gold catalyst derived from SAu_{15}, SAu_{5-6} sols and formed by DPU technique are shown in Figs. 3–5, respectively. On these three differently prepared Au/TiO_2 series the effect of the TiO_2 morphology on the temperature of the 50% conversion in 2–3 runs after different treatments are summarized in Table 4.

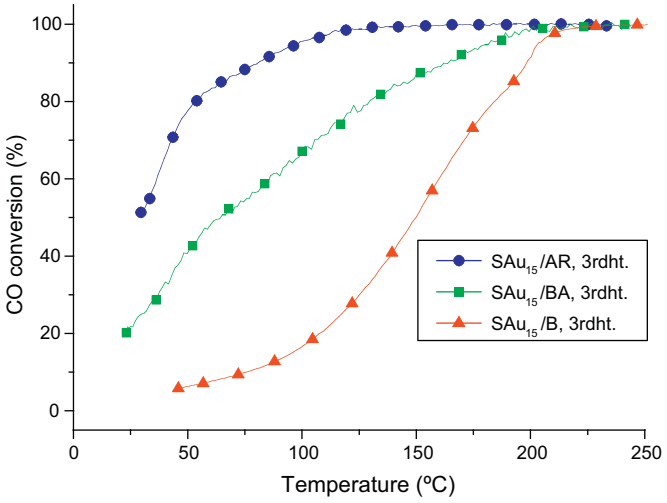

Fig. 3. CO conversion curves of SAu_{15}/AR (●), SAu_{15}/BA (■) and SAu_{15}/B (▲) after calcination at 400 °C in air for 1 h (catalyst weight: 60 mg, reaction mixture flow rate: 35 ml/min).

Among the SAu_{15}/TiO_2 samples the order of CO oxidation activity after calcination at 400 °C was SAu_{15}/AR > SAu_{15}/BA > SAu_{15}/B. The Au particle size was about the same on the AR and B support (on BA it was not measured) whereas the TiO_2 particle size were different. Accordingly, the following order of the length of the Au–TiO_2 perimeter was supposed: SAu_{15}/BA > SAu_{15}/B > SAu_{15}/AR, however, no information is available about the distribution of Au/brookite and Au/anatase interfaces in SAu_{15}/BA. It seems that the Au–brookite perimeter was less active than Au–anatase in the SAu_{15}/TiO_2 samples.

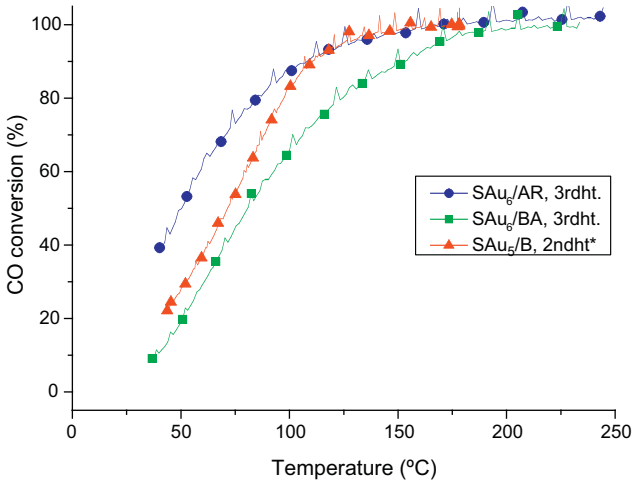

Fig. 4. CO conversion curves of SAu_6/AR (●), SAu_6/BA (■) and SAu_5/B (▲) after calcination at 400 °C in air for 1 h in the first stable or the last measured (*) heating cycles (the 2nd or 3rd) (catalyst weight: 30 mg, reaction mixture flow rate: 27.5 ml/min).

Table 4
Temperature of 50% CO conversion in CO oxidation of different samples after different treatments (the heating–cooling cycles were repeated 2–3 times, if $T_{50\%}$ changed, a region is given for that).

Samples	Temperature of 50% CO conversion, $T_{50\%}$ (°C)				
	As prepared	After reaction, 150 °C/1 h		After calcination, 400 °C/air/1 h	
	1st heating up	Heating up	Cooling down	Heating up	Cooling down
SAu_{15}/AR	–	–	–	44 → 30	33 → 22
SAu_{15}/BA	–	–	–	74 → 64	61 → 87
SAu_{15}/B	–	–	–	157 → 150	141 → 132
SAu_6/AR	–	–	–	35 → 51	35 → 51
SAu_6/BA	–	–	–	75 → 80	79
SAu_5/B	–	–	–	90 → 73	73
DPUAu/AR	53	3	3	3 → 6	8 → 10
DPUAu/BA	53	1 → 2	4 → 5	(−26) → (−4)	(−24) → (−1)
DPUAu/B_1	52	21 → 20	31 → 28	74 → 70	82 → 82
DPUAu/B_2	51	22 → 19	34 → 28	47 → 26	43 → 34

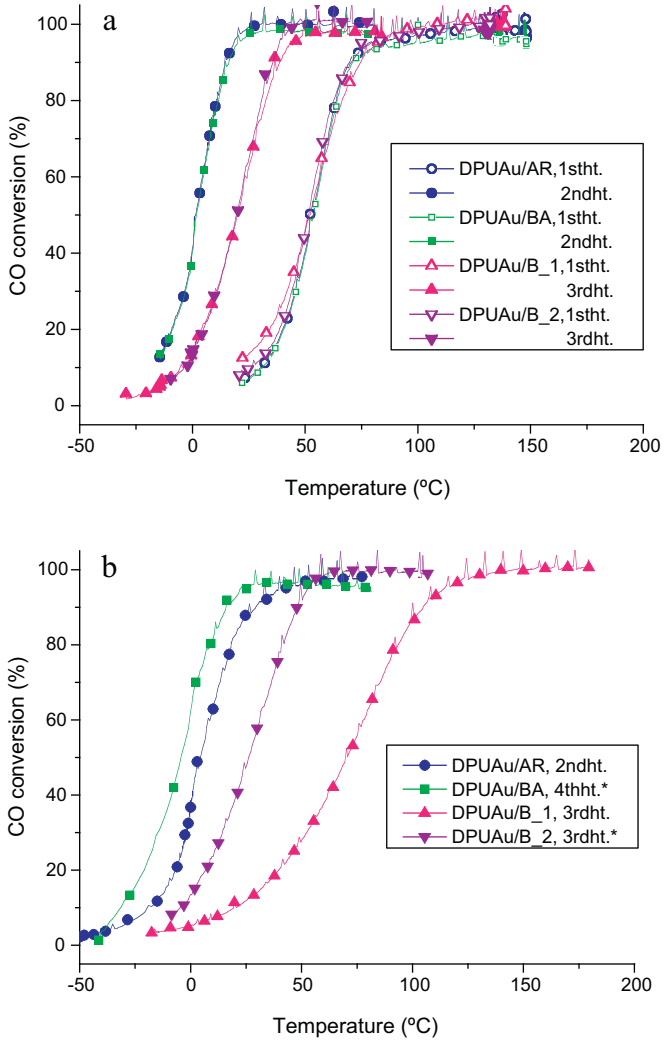

Fig. 5. CO conversion curves of DPUAu/AR (●), DPUAu/BA (■), DPUAu/B_1 (▲) and DPUAu/B_2 (▼) samples. (a) Without pretreatment (1st heating up) and after 1 h reaction at 150 °C the first stable heating up cycle (the 2nd or 3rd) and (b) after subsequent treatment at 400 °C in air for 1 h the first stable or the last measured (*) heating up cycle (the 2nd, 3rd or 4th) (catalyst weight: 30 mg, reaction mixture flow rate: 27.5 ml/min).

The SAu_{5-6}/TiO_2 samples showed somewhat different activity order (SAu_{15}/AR > SAu_{15}/B > SAu_{15}/BA) than the SAu_{15}/TiO_2 ones between the different TiO_2 polymorphs supported samples. However, the higher specific activity of the Au–anatase than that of the Au–brookite perimeter can be deduced also from this comparison, because SAu_5/B must have had the longest Au–TiO_2 perimeter regarding its smallest Au size and that SAu_6/BA contains large fraction of big Au particles. For the comparison of SAu_{5-6}/TiO_2 and SAu_{15}/TiO_2 series, beside the Au size differences, the 70% less contact time in the catalytic measurements of SAu_{5-6}/TiO_2 samples must be taken into account.

For the DPU originated samples the activity order related to the TiO_2 crystalline phase was AR ≈ BA > B before calcination at 400 °C ($T_{50\%}$ of DPUAu/B is higher by about 25 °C). After calcination at 400 °C the activity followed the order BA > AR ≫ B ($T_{50\%}$ of DPUAu/B is higher by about 30–10 and 70–30 °C). The two analogous DPUAu/B samples were similarly active and stable in the repeated catalytic runs before pre-treatment. However, their activity differed after calcination and the difference increased in the repeated runs because one of them was activated. DPUAu/AR was quite stable in both states. In the first catalytic run the as prepared samples were less active than after conditioning in the reaction at 150 °C. The subsequent calcination at 400 °C did not change the activity of DPUAu/AR, activated DPUAu/BA (that activation could not be maintained in the repeated cycles), deactivated DPUAu/B_2 slightly and significantly deactivated DPUAu/B_1 catalysts. The highly dispersed, but possibly not fully reduced Au in the as prepared DPUAu/TiO_2 seemed to be less active than the reduced, less dispersed Au in the case of AR and BA supported calcined samples. For the B supported samples this could not be stated confidently, because the two analogous catalysts behaved differently. DPUAu/B_1 was less active after calcination than in as prepared state on the contrary that it contained highly dispersed gold.

The explanation of all the details of the catalytic behaviour of the differently prepared and treated samples is not easy, especially in case of the BA supported systems. The distribution of Au particles between anatase and brookite phase particles could not be controlled in the as prepared state and it may have changed during the different treatments. On the other hand the determination of the decisive Au particle size was somewhat uncertain in case of BA supported DPU sample, since it was difficult to recognise Au in the TiO_2 network. However, based on the results presented we can conclude that as compared to the pure brookite supported gold catalysts (Au/B), in the Au/Degussa P25 (Au/AR) systems in case of all three types of Au introduction (i) the Au particle size was about the same or significantly larger, and (ii) the Au–TiO_2 perimeter should have been smaller based on (i) and that the pure brookite consisted of somewhat smaller crystallites (23 nm) than Degussa P25 (34 nm anatase, 52 nm rutile). The larger Au size and the shorter perimeter on Degussa P25 should provide lower CO oxidation activity. On the contrary the Degussa P25 supported systems were significantly more active than the corresponding pure brookite supported ones. We regard this as a strong indica-

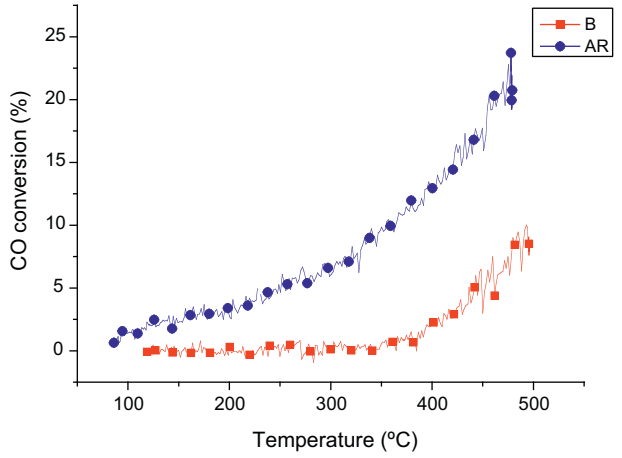

Fig. 6. CO conversion curves of AR (●) and B (■) type TiO_2 (catalyst weight: 50 mg, reaction mixture flow rate: 27.5 ml/min).

tion of the possible larger intrinsic activity of Au–TiO_2 perimeter in Au/AR, so of the Au–anatase perimeter (which is surely more abundant and possibly more but at least not less active [29–32] than Au–rutile interface in Au/AR) compared to the Au–brookite one.

The reasons of the lower activity of the Au–brookite is not revealed, yet, it requires further investigations. The different properties of the TiO_2 polymorphs, as various surface structure, surface enthalpy, differing isoelectronic point, surface hydroxyl concentration, may influence the Au particle formation (DPU preparation) or deposition (sol adsorption) resulting in morphological differences at the Au–TiO_2 interface, which may be differently modified further during pretreatments and catalytic reaction. The different physical and electronic properties of the different phase titania such as band gap, potential of the bottom of conduction band and oxygen binding energy may affect the charge transfer between gold and titania [40], and the mobility of oxygen, the abundance of oxygen vacancies on TiO_2 surface affecting that way the CO activation on gold and O_2 activation on gold and titania.

The own CO oxidation activity of AR and B was measured to find a direct chemical and catalytic consequence of the different properties. Fig. 6 shows the low activity of both AR and B after calcination, however, AR performed significantly higher conversion than B, in spite of having only half of the surface area of the less active brookite (B).

4. Conclusions

The structure and catalytic activity of gold nanoparticles supported on different polymorphs of TiO_2 have been investigated. Pure brookite, brookite–anatase (45:55) and anatase–rutile (85:15) mixtures were compared as supports of Au/TiO_2.

Gold was deposited both by adsorption of Au colloids of about 6 and 15 nm mean diameter and by deposition precipitation (DP) method using urea providing Au particles smaller than 5 nm in size.

Although the size of Au particles on brookite support was smaller or similar, the estimated Au–TiO_2 perimeter larger than on anatase-containing supports, on the latter the activity of CO oxidation was unexpectedly higher. This is explained by difference between the Au-brookite and Au-anatase interface developed and the Au–anatase perimeter seems to be significantly more active in CO activation than the Au–brookite perimeter. The difference in activity should be originated from the different structural, physical and chemical properties of the uppermost oxide layer making interface with gold determined by the crystal structure of TiO_2.

Acknowledgements

The authors are thankful to Dr. A. Kocsonya (KFKI Research Institute for Particle and Nuclear Physics, HAS) for XRF measurements, Dr. I. Sajó and Dr. M. Hegedűs (Chemical Research Center, HAS) for XRD and BET measurements, respectively, and to Prof. T.K. Varadarajan (NCCR IIT Madras) for valuable discussions. The financial help of the National Science and Research Fund (OTKA) grant # K 68052, NNF 78837 and the Indo-Hungarian intergovernmental S & T co-operation programme # OMFB-00741/2008 and Department of Science and Technology, Newdelhi for the Indo-Hungarian project # DST/INT/HUN/P-2/06 are greatly acknowledged. The research was also supported by the COST D36/003/2006 program.

References

[1] J.Y. Park, C. Lee, K.W. Jung, D. Jung, Bull. Korean Chem. Soc. 30 (2009) 402.
[2] M. Koelsch, S. Cassaignon, J.F. Guillemoles, J.P. Jolivet, Thin solid films 403 (2002) 312.
[3] A.D. Paola, M. Bellardita, R. Ceccato, L. Palmisano, F. Parrino, J. Phys. Chem. C 113 (2009) 15166.
[4] M.R. Ranade, A. Navrotsky, H.Z. Zhang, J.F. Banfield, S.H. Elder, A. Zaban, P.H. Borse, S.K. Kulkarni, G.S. Doran, H.J.P. Whitfield, Natl. Acad. Sci. U.S.A. 99 (2002) 6476.
[5] M. Haruta, T. Kobayashi, H. Sano, N. Yamada, Chem. Lett. (1987) 405.
[6] M. Haruta, Catal. Today 36 (1997) 153.
[7] A. Wolf, F. Schüth, Appl. Catal. A 226 (2002) 1.
[8] M. Comotti, W. Li, B. Spliethoff, F. Schüth, J. Am. Chem. Soc. 128 (2006) 917.
[9] N. Weiher, E. Bus, L. Delannoy, C. Louis, D.E. Ramaker, J.T. Miller, J.A. van Bokhoven, J. Catal. 240 (2006) 100.
[10] A.M. Venezia, F.L. Liotta, G. Pantaleo, A. Beck, A. Horváth, O. Geszti, A. Kocsonya, L. Guczi, Appl. Catal. A: Gen. 310 (2006) 114.
[11] A. Horváth, A. Beck, A. Sárkány, Gy. Stefler, Zs. Varga, O. Geszti, L. Tóth, L. Guczi, J. Phys. Chem. B 110 (2006) 15417.
[12] L. Guczi, A. Beck, K. Frey, Gold Bull. 42 (2009) 5.
[13] J. Guzman, B.C. Gates, J. Am. Chem. Soc. 126 (2004) 2672.
[14] X. Wu, L. Senapati, S.K. Nayak, A. Selloni, M. Hajaligol, J. Chem. Phys. 117 (2002) 4010.
[15] M. Valden, X. Lai, D.W. Goodman, Science 281 (1998) 1647.
[16] M. Haruta, Cattech 6 (2002) 102.
[17] M. Manzoli, A. Chiorino, F. Boccuzzi, Surf. Sci. 532–535 (2003) 377.
[18] L. Fu, N.Q. Wu, J.H. Yang, F. Qu, D.L. Johnson, M.C. Kung, H.H. Kung, V.P. Dravid, J. Phys. Chem. B 109 (2005) 3704.
[19] N. Lopez, T.V.W. Janssens, B.S. Clausen, Y. Xu, M. Mavrikakis, T. Bligaard, J.K. Norskov, J. Catal. 223 (2004) 232.
[20] G. Mills, M.S. Gordon, H. Metiu, Chem. Phys. Lett. 359 (2002) 493.
[21] R. Meyer, C. Lemire, Sh. Shaikhutdinov, H.-J. Freund, Gold Bull. 37 (2004) 72.
[22] N. Lopez, J. Norskov, J. Am. Chem. Soc. 124 (2002) 11262.
[23] M. Mavrikakis, P. Stoltze, J.K. Norskov, Catal. Lett. 64 (2000) 101.
[24] G.C. Bond, D.T. Thompson, Gold Bull. 33 (2001) 41.
[25] J.J. Pietron, R.M. Stroud, D.R. Rolison, Nano Lett. 20 (2002) 545.
[26] M.M. Schubert, S. Hackenberg, A.C. van Veen, M. Muhler, V. Plzak, R.J. Behm, J. Catal. 197 (2001) 113.
[27] A. Sanchez, S. Abbet, U. Heiz, W.-D. Schneider, H. Hakkinen, R.N. Barnett, U. Landman, J. Phys. Chem. A 103 (1999) 9573.
[28] Q. Fu, H. Saltsburg, M. Flytzani-Stephanopoulos, Science 301 (2003) 935.
[29] K.Y. Ho, K.L. Yeung, Gold Bull. 40 (2007) 15.
[30] M. Comotti, C. Weidenthaler, W. Li, F. Schüth, Topics Catal. 44 (2007) 275.
[31] W. Yan, B. Chen, S.M. Mahurin, S. Dai, S.H. Overbury, Chem. Commun. (2004) 1918.
[32] W. Yan, B. Chen, S.M. Mahurin, V. Schwartz, D.R. Mullins, A.R. Lupini, S.J. Pennycook, S. Dai, S.H. Overbury, J. Phys. Chem. B 109 (2005) 10676.
[33] F. Arena, P. Famulari, G. Trunfio, G. Bonura, F. Frusteri, L. Spadaro, Appl. Catal. B 66 (2006) 81.
[34] N. Dimitratos, A. Villa, C.L. Bianchi, L. Prati, M. Makkee, Appl. Catal. A 311 (2006) 185.
[35] R.J.H. Grisel, P.J. Kooyman, B.E. Nieuwenhuys, J. Catal. 191 (2000) 430.
[36] D.H. Lee, J.G. Park, K.J. Choi, H.J. Choi, D.W. Kim, Eur. J. Inorg. Chem. 2008 (2008) 878.
[37] A. Pottier, C. Chaneac, E. Tronc, L. Mazerolles, J.P. Jovilet, J. Mater. Chem. 11 (2001) 1116.
[38] R. Zanella, S. Giorgio, C.R. Henry, C. Louis, J. Phys. Chem. B 106 (2002) 7634.
[39] A. Beck, A. Horváth, Z. Schay, Gy. Stefler, Zs. Koppány, I. Sajó, O. Geszti, L. Guczi, Topics Catal. 44 (2007) 115.
[40] S.D. Mo, W.Y. Ching, Phys. Rev. B 51 (1995) 13023.